Journal of Molecular Liquids 311 (2020) 113328

Contents lists available at ScienceDirect

Journal of Molecular Liquids

journal homepage: www.elsevier.com/locate/molliq

Nanosized Titania-Nickel mixed oxide for visible light photocatalytic activity

Saravanan Rajendran [a,*], Devaraj Manoj [b], J. Nimita Jebaranjitham [c], Baskaran Ganesh Kumar [d,e], G. Bharath [f], Fawzi Banat [f], Jiaqian Qin [g], S. Vadivel [h], F. Gracia [i]

[a] Faculty of Engineering, Department of Mechanical Engineering, University of Tarapacá, Avda, General Velasquez, 1775 Arica, Chile
[b] Key laboratory of Material Chemistry for Energy Conversion and Storage, Ministry of Education, School of Chemistry and Chemical Engineering, Huazhong University of Science and Technology, Wuhan 430074, China
[c] PG Department of Chemistry, Women's Christian College (An Autonomous Institution Affiliated to University of Madras), College Road, Chennai 600 006, Tamil Nadu, India
[d] Department of Chemistry, P.S.R. Arts and College (Affiliated to Madurai Kamaraj University, Madurai), Sivakasi, TN, India
[e] Department of Science and Humanities, P.S.R. Engineering college (Affiliated to Anna University, Chennai), Sivakasi, TN, India
[f] Department of Chemical Engineering, Khalifa University, P.O. Box 127788, Abu Dhabi, United Arab Emirates
[g] Research Unit of Advanced Materials for Energy Storage, Metallurgy and Materials Science Research Institute, Chulalongkorn University, Bangkok 10330, Thailand
[h] Department of Chemistry, PSG College of Technology, Coimbatore 641004, India
[i] Department of Chemical Engineering, Biotechnology and Materials, University of Chile, Beauchef 851, 6th floor, Santiago, Chile

ARTICLE INFO

Article history:
Received 4 March 2020
Received in revised form 3 May 2020
Accepted 7 May 2020
Available online 11 May 2020

Keywords:
Visible light
Photocatalyst
Methyl Orange
Nanomaterial
Degradation

ABSTRACT

Colourful dyes are primarily used in the textiles, toys, food, inks, paper and plastics. These dyes are water soluble and contaminate the water. The dyes are not bio-degradable and sustain in the water for long time create diseases like bladder tumour and chromosomal damage. Hence dyes are the major cause of pollution and must be removed from domestic and drinking water. The photocatalysts are energy-less technology for dye degradation and expected to solve clean water problems. Most of the photocatalysts are metal oxides and absorbed in the ultra violet region. But, sun light mostly consists of visible light, hence to use the sunlight effectively the absorption spectrum of the photocatalysts must be tuned to the visible region. Herein, we proposed visible light absorbed new TiO_2/NiO nanocomposite for methyl orange dye degradation. The integration of NiO modified the TiO_2 nanocomposite UV absorption spectrum into visible light region. The photocatalyst was prepared using mechano-thermal method and characterised using PXRD, TGA, FT-IR, HR-TEM, EDS, UV, PL and DRS methods. The photocatalytic property was explored using the degradation of methyl orange and compared the activity with different time intervals and wide range of pH. Within 60 min of irradiation, 98% of degradation was observed. Similarly, at all pH range more than 50% of degradation was observed, but the best performance (98%) was observed at pH = 7 (neural). Thus, the TiO_2/NiO nanocomposite catalyst was effective in neutral, acidic and basic polluted water treatment. The synthesized TiO_2/NiO nanocomposite is tuneable to visible light and degrade the methyl orange dye in all pH range.

1. Introduction

In recent years, the wide scale of manufacturing divisions are accumulating and causes a lot of harmful effects in the environment. Predominantly, fabric industrial units regularly utilizes toxic or destructive organic colourants for customised dying process [1]. The outlet of dying sewages were generally untreated and immediately passed through our drinking aquatic bodies that lead to engender numerous diseases for human and all other living species [1,2]. The investigators are most passionate to discover and elucidate the above stated water problem [1–3]. In this connection, there are numerous physical and chemical methods emerging to resolve the waste water problem.

Associated with other water-purification management methods, photocatalysis is an exclusive technology since it is simple to operate and valuable proficiency via low-cost process. Furthermore, in the recent times, nanocatalysts expressed an energetic characteristics to reduce the organic contaminations [4]. Particularly, wide band gap nano semiconductors (TiO_2, ZnO, SnO_2, CeO_2 and NiO) show an outstanding photocatalytic degradation capability over toxic organic pollutants [5]. When compared with other photocatalytic materials, nanosized titania (TiO_2) has exhibited greater degradation ability of textile dyes due to its intrinsic positive band position which effectively generated more electrons and holes, leads to abolish the organic colourant through the exposure of UV light. The reality of TiO_2 has a large bandgap material

* Corresponding author.
E-mail address: saravanan3.raj@gmail.com (S. Rajendran).

https://doi.org/10.1016/j.molliq.2020.113328
0167-7322/

(3.2 eV) which shows an inauspicious nature to accomplish the textile dyes under the exploitation of visible source [5,6].

Based on the prior literatures, it has been realised that the postponement of electron-hole recombination process improves the photocatalytic competency of the catalyst. In this relation, hybrid metal oxides were attracted a lot of researchers due to its enhanced photocatalytic performance. On the other hand, the hybrid or coupled materials possess new potential applications like optoelectronic, electrochemical devices, sensors, solar cells, photocatalysis and biological imaging, etc. [4–12]. When matched with pure TiO_2 performance, the coupled or doped systems were exposed higher methyl orange and methylene blue degradation rate, because of the presence of synergistic effect and higher surface area [6,13]. Recent times, TiO_2 incorporated with other different bandgap systems (TiO_2-CeO_2, TiO_2- SnO_2, TiO_2-CuO, TiO_2-CdO etc.,) were exhibited active photocatalytic capacity under visible light or enriched UV light degradation responses due to the addition of other system. The coupled materials have the capability to engross visible light source and directed to create more photogenerate electrons and holes. Further, the photogenerated electrons and holes transfer through hopping mechanism due to newly generated larger band. [14,15]. However, some of the previous reports described when TiO_2 coupled with NiO converts TiO_2 to visibly active material [16,17]. The results are contrary, due to the existing dual material that possess large bandgaps ($TiO_2 = 3.2$ eV and $NiO = 3.6$ eV). The TiO_2 and NiO materials are unable to absorb the visible light, but absorb in ultraviolet region due to wide band gap of the materials. Therefore, we need deep understanding of TiO_2-NiO system and its visible light induced photocatalytic mechanism is still confused to explain.

In the present manuscript, TiO_2-NiO nanocomposite system was synthesized by novel method via sol-gel combined with mechano-thermal synthesis process. The obtained TiO_2-NiO properties were characterised by different examination tools such as PXRD, TEM and XPS and their observed results were discussed herein. In addition, the core theme of existing study is to recognize the visible light tempted photocatalytic degradation mechanism of nano TiO_2-NiO co-catalyst. We analysed the photocatalytic viability of TiO_2/NiO composite using degradation of methyl orange. It was found that NiO/TiO_2 acted as a co-catalyst for methyl orange degradation. Within 60 min of irradiation, 98% of degradation was observed. Similarly, at all pH range more than 50% of degradation was observed, but the best performance (98%) was observed at pH = 7 (neural). At the end, it has been proposed that the formation of p-n junction along with Ni^{3+} states promotes more generation of electrons which prevent electrons-holes recombination. The suppressed recombination endorses the prepared system has an effectual influence to participate under visible light MO degradation processes.

2. Experimental section

2.1. Materials

The following chemicals, nickel acetate, titanium tetra isopropoxide and citric acid were purchased (Sigma-Aldrich) and used without further purification. Similarly, analytical grade methyl orange (for photocatalytic analysis) and isopropyl alcohol were purchased. Moreover, Milli-Q water used during the preparation of TiO_2-NiO and photocatalytic experiments.

2.2. Synthesis of nanosized TiO_2-NiO co-catalyst

The utilization of modern synthetic technique was performed to prepare nanosized TiO_2-NiO co-catalyst which was reported in our previous literature [18]. At first, the sol-gel method was considered to synthesize and purify the pre-calcinated TiO_2 powder. Thereafter, mechanothermal synthesis was instigated to attain the nanosized TiO_2-NiO co-catalyst. The preparation stages of co-catalyst were divided into two parts and which was defined in short as follows: 30 ml of prepared titanium tetra isopropoxide was liquified with 150 ml of prepared isopropyl alcohol in a fume-cupboard which was placed under constant stirring condition. Additionally, 0.5 M of aqueous citrate solution was prepared and gradually added in the prepared solution, then the reaction solution was turned into gel and collected. Then the solution was subjected in a muffle furnace at 150 °C for 30 min. During the reaction time, the gel was transformed to a pre-synthesized TiO_2 powder material. After this, the mechanothermal process was prompted to prepare TiO_2-NiO co-catalyst. In this method, the raw materials (nickel acetate of 100 mg of and 900 mg of pre-synthesized TiO_2 powder material attained from the above sol-gel process) were mixed and ground with agate pestle and mortar for ~3 h. The dehydration and decomposition temperature of organic substances from the obtained mixed powder were analysed through TGA measurement. The samples were grounded and calcined in a muffle furnace at 450 °C and digested for 1 h. Then the calcined material was slowly cooled down to room temperature (4 °C/min), which in turn the process assisted to produce nanosized mesoporous TiO_2-NiO co-catalyst.

2.3. Photocatalytic experiment

The theme of the present work is focused visible light degradation of organic dyes. In this scenario, aquatic methyl orange solution was utilised as a standard organic dye (different pH level). The photocatalytic testing procedure and their steps were defined in our previous reports [19,20]. In the present analysis, the visible light was generated from SCIENCETECH (SF300 B)-AM 1.5G. During the photocatalytic activity, different dosage of catalysts (25 to 200 mg) were monitored. Dark and visible light exposed methyl orange solutions were scrutinized by UV–vis absorption spectrophotometer and GCMS (Perkin Elmer Autosystem).

2.4. Instrumentation

The thermal decomposition of the as-synthesized materials was analysed by Thermogravimetry (TGA-TA Instruments TGA Q50) with continuous flow of N_2 with a heating rate of 10 °C/min. The functional groups present in the nanocomposite were examined by Fourier transform infrared (FT-IR) spectroscopy (Thermo scientific, Nicolet IS 50). The powder samples made as pellet using KBr high pressure technique and measured with the range in-between 4000 cm^{-1} to 400 cm^{-1}. The nanocomposite crystallinity, phase and crystal structure of the materials were identified by X-ray diffraction using D5000 diffractometer, Siemens, USA and measured with $CuK_{\alpha 1}$ ($\lambda = 1.5406$ Å) irradiation. The synthesized particle size and overall morphology were calculated by a high-resolution transmission electron microscope (HR-TEM), FEI TITAN G^2 80–300 (operated at 300 keV) and EDS analysis also carried out with same. The composite chemical composition of the synthesized nanoparticles was predicted using X-ray fluorescence (XRF, EDX-720, Shimadzu). The X-ray photoelectron spectroscopic measured using Thermo Scientific Escalab 250Xi. The emission measurements were carried out using a Perkin Elmer spectrofluorometer LS-55. The absorbance spectra of the prepared materials and degraded dye samples were obtained using a Perkin Elmer Lambda 35 spectrometer.

3. Result and discussion

In the thermogravimetric consequence of pre-synthesized TiO_2 and mixed raw materials, the co-catalyst has subjected to find the decomposition physisorbed water, organic spices and suitable calcination temperature for the formation of pure and hybrid oxide system and the corresponding result was described in Fig. 1.

In Fig. 1, the result was perceptibly quantified that there are two most important weight losses occured from the TGA curve of both pre-synthesized samples. Preliminary, weight loss (~ 4% to 6%) of both samples was happened at 70 °C to 100 °C, which directs the surface of

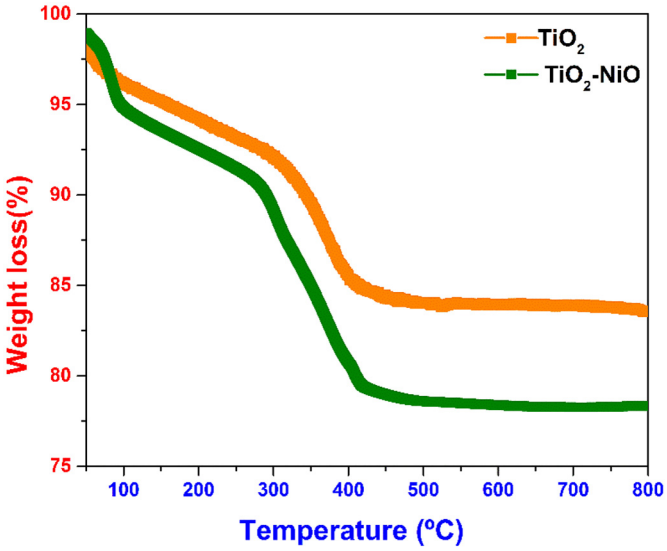

Fig. 1. TGA result of the prepared materials.

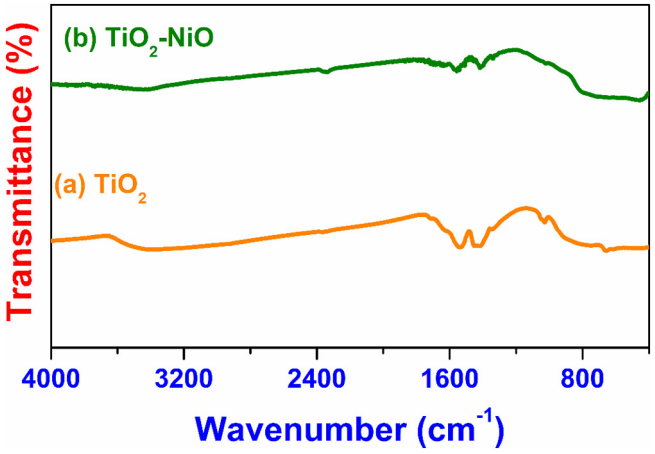

Fig. 2. FT-IR spectrum of the prepared materials.

the pre-synthesized samples that have water molecules evaporated in this temperature range. Further, the secondary predominant weight loss (~15% to 22%) shows in 100 °C to 410 °C, point out the decomposition of organic ingredient from the pre-synthesized samples. However, the TGA curve of as-prepared co-catalyst sample was experienced with more weight losses (~22%) at slightly higher temperature when compared with pre-synthesized of pure TiO_2 (~15%) system due to the existence of two different materials TiO_2 and NiO. After that, there is no weight loss observed between 410 °C and 800 °C which reflected the formation of crystallization achieved after 410 °C. Hence, in this current study, the optimum calcination temperature was fixed at 450 °C based on the TGA curve. After calcination process, the obtained yields of co-catalyst and its chemical composition and structure purity were described via XRF and XRD measurements.

The XRF upshot was indisputably agreed that the prevailing elements viz., NiO and TiO_2 were originated from the synthesized co-catalyst scheme and their consistent quantities were shown in the Table 1.

Additionally, the XRD (the figure in the Supporting information – SI 1) of the prepared co-catalyst has exhibited the anatase-tetragonal structure of TiO_2 in joint with a cubic Ni^{2+}/Ni^{3+} peak seemed at 43.18° and their resultant crystallite size, structural parameter was depicted in Table 1. Therefore, the XRD result proved that the co-catalyst was in existence with mixed hybrid structure which directed to generate several interfaces [21].

The presence of functional group of prepared catalyst was analysed by FT-IR spectra and their corresponding consequence was displayed in Fig. 2. The hydroxyl (OH), carbonyl (C=O), and metal oxide (M-O) functional bonds are diagnosed from pure TiO_2 system which are appeared at 3445 cm^{-1} (OH), 1558 cm^{-1} (C=O), 1420 cm^{-1} (C=O) and 660 cm^{-1} (O-Ti-O). Similarly, the co-catalyst system was shown all the above stretching vibration modes along with O-Ni-O seemed at 570 cm^{-1} [22]. Hence, the FT-IR spectra were proved the existing functional group of the prepared system which demonstrated the formation of co-catalyst.

The prepared co-catalyst size and shape evidence were predicted with the reflection of TEM micrographs. The TEM image (Supporting information – SI 2, Fig. 2a) has showed that the spherical shaped tiny NiO nanoparticles were reliably dispersed over the surface of TiO_2. From the HR-TEM image, shown in Supporting information – SI 2, Fig. 2b, the d-spacing value of attained grains or crystallites were completely analysed. The pattern has clearly indicated that 0.352 nm (101), 0.243 nm (103) and 0.237 nm (004) planes of TiO_2 (Anatase-Tetragonal, JCPDS NO: 21-1272) including 0.241 nm (111), 0.208 nm (200) and 0.147 nm (220) plane of NiO (Cubic, JCPDS NO: 21-1272). The HR-TEM results were unambiguously complemented by XRD analysis. In HRTEM analysis, the decorated circular portion has been specified after the accumulation of NiO nanoparticles into TiO_2 surface. The nanocomposite formation has created dislocation and more interfaces are commanded to generate line defect which offers oxygen vacancies [23]. The EDS pattern (Supporting information – SI 2, Fig. 2c) has apparently conveyed that the synthesized co-catalyst consisted of Ni, Ti, O and Cu elements.

The composition and their oxidation state of surviving elements in the prepared co-catalyst were examined by XPS measurement. The XPS pattern has recognized the presence of Ti, Ni, and O elements and their binding energies were totally resolved through C 1 s (284.6 eV) as a reference. The XPS images (Supporting information – SI 3) and their conforming data were organized in Table 2. The HR-XPS co-catalyst scheme comprised with two symmetric peaks of titania (Ti

Table 1
XRF and XRD outcome of the prepared materials.

Prepared sample	XRF		XRD					
			Structure (JCPDS No.) and lattice parameter		Crystallite size (nm)		Quantitative Analysis – Rietveld	
	TiO_2 (%)	NiO (%)	TiO_2	NiO	TiO_2	NiO	TiO_2 (%)	NiO+ (%)
Pure TiO_2	100	------	Anatase-tetragonal (21–1272) a = b = 3.791 Å and c = 9.508 Å	-----	18.1	----	100	-----
TiO_2-NiO co-catalyst	95.5	4.5	Anatase-tetragonal (21–1272) a = b = 3.797 Å and c = 9.522 Å	Cubic (47–1049) a = 4.190 Å	18.2	7.3	95.10	4.90

Table 2
XPS and UV–vis outcome of the prepared materials.

Sample	XPS					UV–Vis absorption
	Existing elements	Start binding energy eV	End binding energy eV	Area CPS. eV	Atomic %	Bandgap energy calculated from Tauc Plot
Pure	Ti_2p	466	452	36,418.3	29.29	3.18 eV (390 λ)
TiO_2	O1s	534	525	32,226.78	70.71	
TiO_2-NiO co-catalyst	Ti2p	464	450	48,845.82	27.35	2.89 eV (429 λ)
	O1s	533	527	44,723.81	68.29	
	Ni2p	886	850	19,968.11	4.36	

2p) were perfectly tailored with the use of Gaussian functions and their variation is 5.7 eV that was referenced to Ti^{4+} state. On the other hand, Ni 2*p* has exhibited Ni^{3+} and Ni^{2+} states and the O 1 s peaks were associated with NiO, Ni_2O_3, TiO_2 and hydroxyl in the co-catalyst. Interrelated with pure TiO_2 analysis, the co-catalyst possess lower binding energies that recommend surface modifications which provided more interfaces [24]. Hence, the XPS results suggested that clearly the Ni^{3+} was associated in TiO_2- NiO co-catalysts system.

The core strategy of this present study, effectively prompting the photocatalytic activity of TiO_2 nanostructure by the way of combination of NiO material. In this connection, finding the changes in the optical bandgap of the synthesized co-catalyst is essential due to utilization of specific wavelength of light in the catalytic reaction [25]. The UV–vis absorption spectrum of the prepared materials was shown in Fig. 3. The result of pure material is demonstrated that well crystallinity was identified via the absorption spectrum of pure material, which reflect very sharp edge is at 390 nm. Concurrently, the co-catalyst spectrum was displayed broad edge (410–430 nm) which stated that the prepared co-catalyst contains amorphous materials [26]. The embodied inset figure labelled the optical bandgap of the prepared materials were estimated from Tauc plot [27] and the values are shown in Table 2.

The prepared co-catalyst shows lower bandgap due to established strong interfaces in-between TiO_2 and NiO materials which promotes easier to transfer electrons in the conduction band NiO to TiO_2 [17,28]. For additional intention behind the reason of decreasing the band gap is the survival of line defect and Ni^{3+} ions which are persuading intermediate state between the bandgap of NiO/TiO_2 system [28]. When compared with pure system, the co-catalyst having intermediate state that makes delay for electrons-holes recombination process that reduces the PL intensity (Fig. 4). Concluded from the observation of UV–vis absorption and PL outcomes, during the photocatalytic reaction, the newly created intermediate states are effective and prevent the recombination process [19]. The suppression of recombination process encourage more number of electrons and holes to participate in the TiO_2-NiO catalytic process.

In this study, the competence of visible light photocatalytic reaction of TiO_2-NiO catalyst has been monitored through the examination of methyl orange (MO) degradation. Primarily, the photolysis performance of MO has examined by visible light irradiation (~1 h), and their consistent absorption results recommended that the MO dye has shown no changes in the absorption which postulates that the MO dye has shown a constant photostability. We know that, the pure TiO_2 system has incapable to generate electrons and holes under visible light illumination due to its wide band gap (~3.2 eV). Further, to find the optimal amount of TiO_2-NiO catalyst, a series of MO degradation experiments (concentration of MO is 3×10^{-3} M) were carried out. In these reaction, different quantities of TiO_2-NiO material (from 25 mg to 200 mg of catalyst/L of MO dye) were used for MO degradation. During regular interval of irradiation, the elimination of MO efficiency was calculated, and their corresponding results were shown in Fig. 5a. The removal of MO results conclusively described that the degradation percentage is increased while loading 25 mg to 100 mg of catalysts. After that, the higher dosage (150 mg and 200 mg) shows comparable and slightly decreasing degradation rate. Because, high amount of catalysts reduce the light transmission during the photoreaction [29,30]. Therefore, in the above observation, we optimized 100 mg of TiO_2-NiO catalyst that shows better degradation result while compared with other quantities.

The manufacturing sewage generally have a wide range of pH values and it play a significant role during the degradation reaction.

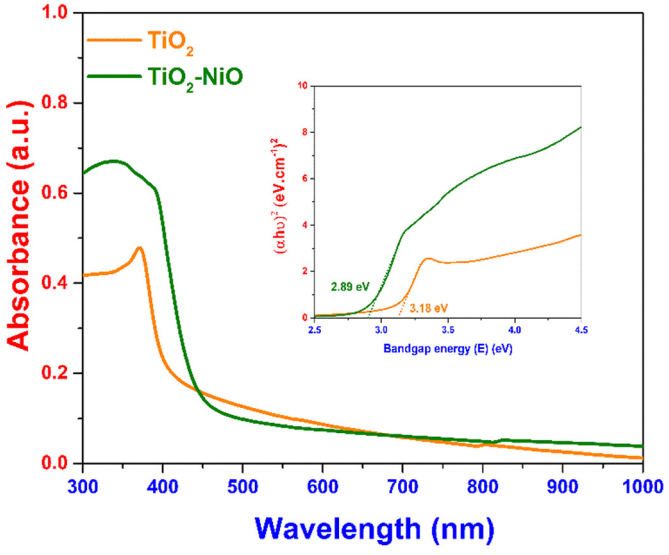

Fig. 3. UV–vis absorption spectrum of the prepared materials (inserted image represented bandgap determination using Tauc plot).

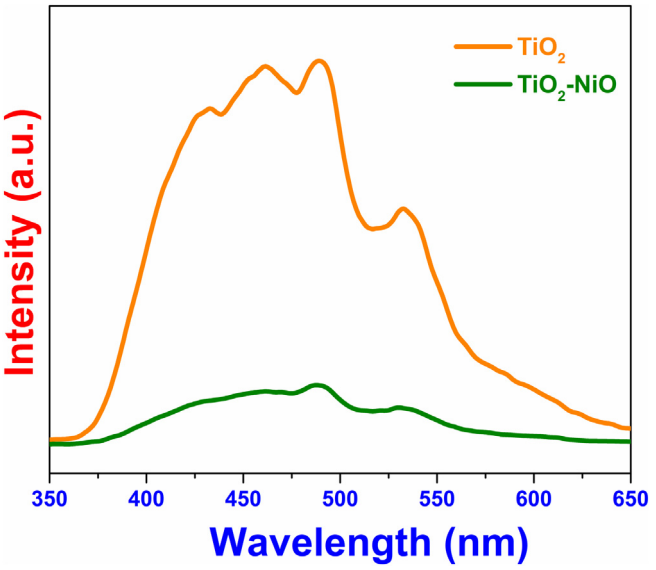

Fig. 4. PL spectrum of the prepared materials.

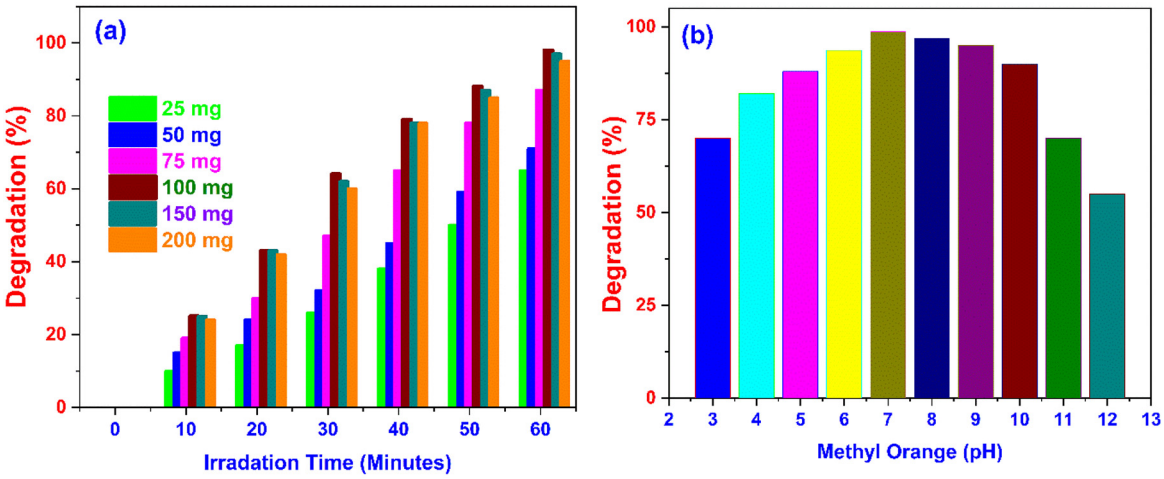

Fig. 5. Photocatalytic degradation of (a) Different quantities of TiO_2-NiO materials and (b) Different pH of MO solution.

Henceforward, attempting with different pH of MO has been carried by evaluating the performance of optimal quantity of prepared TiO_2-NiO catalyst (100 mg) verses different pH value. In Fig. 5b, it clearly exhibits the different pH value effectually influence on the degradation. Based on degradation (acid and alkaline medium) results, pH = 7 displayed higher degradation (98% for 60 min). Because of accumulation of charge on the surface of the catalysts (TiO_2-NiO), it may influence the dispersibility of the reaction suspension. The comparable remark was described in the preceding literatures [29,30].

The pathway diagram and GC–MS results help to clearly identify the intermediates and final outcomes of the photocatalytic reaction (Fig. 6a). The catalyst (TiO_2-NiO) consists of Ti^{4+}, Ni^{2+}, Ni^{3+} states (which were identified by XPS results). The occurrence of NiO and TiO_2 creates the formation of p-n junction and the presence of Ni^{3+}

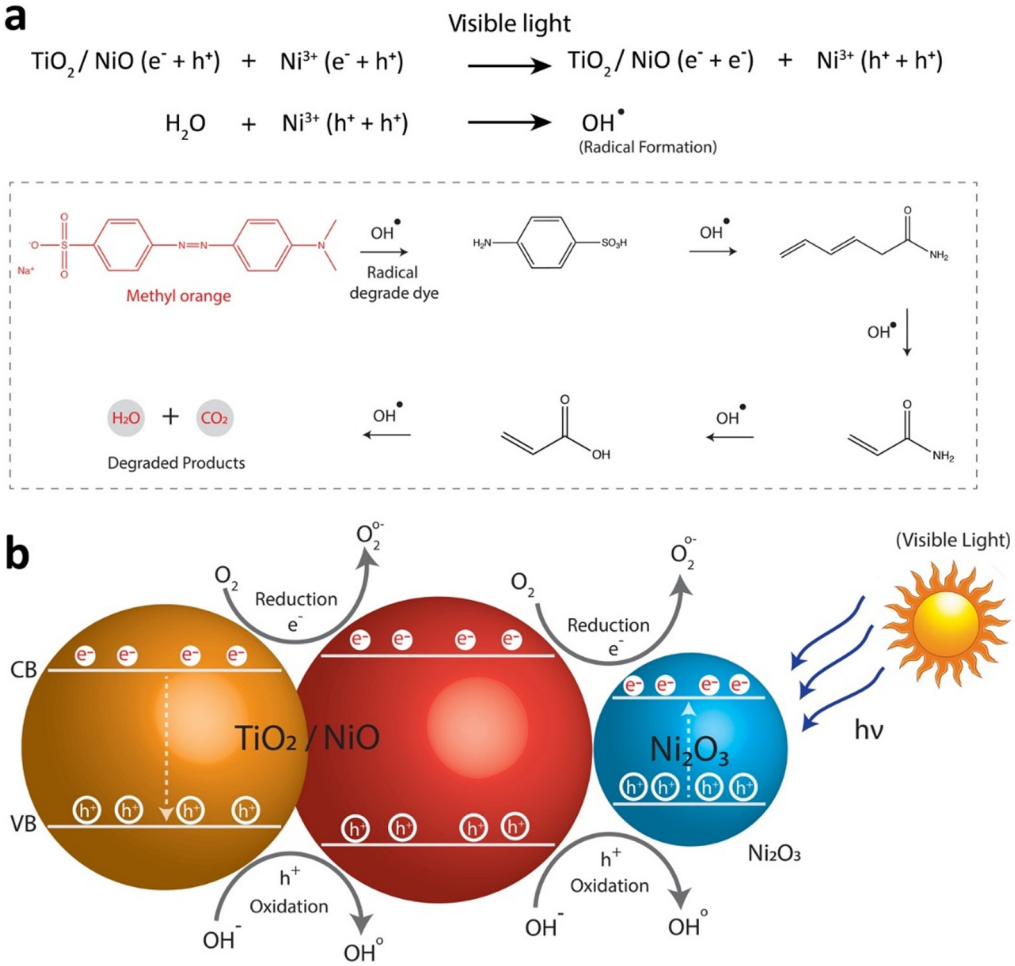

Fig. 6. Photocatalytic degradation of (a) degradation pathway of dye Methyl orange (b) schematic diagram of photo electron-hole generation.

having additional capability to absorb the visible light and initiating the photocatalytic process [31,32]. The schematic representation of photocatalytic degradation of TiO_2-NiO system is shown in Fig. 6b. Furthermore, the persisting Ni^{3+} generates dislocation on the surface of the TiO_2-NiO system which prompts more electrons facilitate during the photocatalytic reaction [31,32]. The dislocation has clearly acknowledged in HR-TEM image (Supporting information – SI 2, Fig. 2b). Hence, the formation p-n junction along with Ni^{3+} states promotes more generation of electrons and prevention of electrons-holes recombination which endorses the prepared system has an effectual influence to participate in visible light MO removal processes.

4. Conclusion

With the intention of tuning UV absorption of TiO_2 to visible region, NiO is integrated and prepared the TiO_2/NiO nanocomposite. The TiO_2/NiO composite was prepared using mechano-thermal method. The NiO integration in TiO_2 was successful and analysed using the UV–visible absorption spectrum, PXRD and TEM analysis. The NiO integration migrated the band gap of TiO_2 nanoparticles from 3.18 eV to 2.89 eV and estimated using Kubelka-Munk conversion. The TEM micrographs showed that TiO_2 and NiO are composited together with signature planes of TiO_2 (1 0 1), (1 0 3), (0 0 4) and NiO (2 0 0), (1 1 1) and (2 2 0). Notably, through XRF analysis, mere 4.5% of NiO integration shifts the TiO_2 absorption to visible spectra. The PXRD analysis exhibited that NiO integration did not alter the crystal structure of TiO_2 (anatase, JCPDS# 21-1272) phase and NiO (JCPDS = 47-1049) has been presented as a cubic phase. The XPS analysis proved that the oxidation state of nickel as 2+, 3+ and titanium as 4+. In summary, synthesized TiO_2/NiO composite, characterised completely and successfully tuned the absorption spectrum to the visible region.

It has been analysed the photocatalytic viability of TiO_2/NiO composite using degradation of methyl orange. It was found that NiO/TiO_2 acted as a co-catalyst for methyl orange degradation. We compared the photocatalytic activity with different time intervals and wide range of pH. Within 60 min of irradiation, 98% of degradation was observed. Similarly, at all pH range more than 50% of degradation was observed, but the best performance (98%) was observed at pH = 7 (neural). Thus, the TiO_2/NiO nanocomposite catalyst was effective in neural, acidic and basic polluted water treatment. The synthesized TiO_2/NiO nanocomposite is tunable to visible light and degrade the methyl orange dye in all pH range. The mechanism of methyl orange degradation was analysed using GCMS analysis. The entire pathway of degradation was followed and identified. We propose that the formation of p-n junction along with Ni^{3+} states promotes more generation of electrons which prevent electrons-holes recombination. The suppressed recombination endorses the prepared system has an effectual influence to participate visible light MO degradation processes.

CRediT authorship contribution statement

Saravanan Rajendran: Writing - original draft, Conceptualization, Methodology, Writing - review & editing, Visualization, Investigation, Software, Validation. **Devaraj Manoj:** Conceptualization, Methodology, Writing - review & editing. **J. Nimita Jebaranjitham:** Conceptualization, Methodology, Writing - review & editing. **Baskaran Ganesh Kumar:** Writing - original draft. **G. Bharath:** Visualization, Investigation, Software, Validation. **Fawzi Banat:** Visualization, Investigation, Software, Validation. **Jiaqian Qin:** Visualization, Investigation, Software, Validation. **S. Vadivel:** Visualization, Investigation, Software, Validation. **F. Gracia:** Visualization, Investigation, Software, Validation.

Declaration of competing interest

No conflict of interest.

Acknowledgements

The authors (S.R., F.G.) acknowledge the support of ANID through the project ANID/FONDAP/15110019. The author (S.R) acknowledge FONDECYT Government of Chile (Project No.: 11170414), for the support to carry out this project.

Appendix A. Supplementary data

Supplementary data to this article can be found online at https://doi.org/10.1016/j.molliq.2020.113328.

References

[1] M. Li, X. Wang, C.J. Porter, W. Cheng, X. Zhang, L. Wang, M. Elimelech, Concentration and recovery of dyes from textile wastewater using a self-standing, support-free forward osmosis membrane, Environ. Sci. Technol. 53 (2019) 3078–3086.
[2] C.X. Liu, et al., Highly efficient photocatalytic degradation of dyes by a copper–triazolate metal–organic framework, Chemistry A European Journals 24 (2018) 16804–16813.
[3] X. Yang, L. Duan, X. Ran, Photocatalytic degradation of organic dyes by a donor–acceptor type conjugated polymer: poly (thiophene-1,3,4-oxadiazole) and its photocatalytic mechanism, Polym. Int. 67 (2018) 1282–1290.
[4] C. Xu, P.R. Anusuyadevi, C. Aymonier, R. Luque, S. Marre, Nanostructured materials for photocatalysis, Chem. Soc. Rev. 48 (2019) 3868–3902.
[5] N. Serpone, A.V. Emeline, Semiconductor photocatalysis-past, present, and future outlook, J. Phys. Chem. Lett. 35 (2012) 673–677.
[6] R. Fagan, D.E. McCormack, D.D. Dionysiou, S.C. Pillai, A review of solar and visible light active TiO_2 photocatalysis for treating bacteria, cyanotoxins and contaminants of emerging concern, Mater. Sci. Semicond. Process. 42 (2016) 2–14.
[7] H. Karimi-Maleh, O.A. Arotiba, Simultaneous determination of cholesterol, ascorbic acid and uric acid as three essential biological compounds at a carbon paste electrode modified with copper oxide decorated reduced graphene oxide nanocomposite and ionic liquid, J. Colloid Interface Sci. 560 (2020) 208–212.
[8] Z. Shamsadin-Azad, M.A. Taher, S. Cheraghi, H. Karimi-Maleh, A nanostructure voltammetric platform amplified with ionic liquid for determination of tert-butylhydroxyanisole in the presence kojic acid, Journal of Food Measurement and Characterization 13 (2019) 1781–1787.
[9] H. Karimi-Maleh, K. Cellat, K. Arıkan, A. Savk, F. Karimi, F. Şen, Palladium–nickel nanoparticles decorated on functionalized-MWCNT for high precision non-enzymatic glucose sensing, Mater. Chem. Phys. 250 (2020), 123042. .
[10] J. Mohanraj, D. Durgalakshmi, R. Ajay Rakkesh, S. Balakumar, Saravanan Rajendran, Hassan Karimi-Maleh, Facile synthesis of paper based graphene electrodes for point of care devices: a double stranded DNA (dsDNA) biosensor, J. Colloid Interface Sci. 566 (2020) (463-462).
[11] Hassan Karimi-Maleh, Marjan Shafieizadeh, Mohammad A. Taher, Francis Opoku, Ephraim Muriithi Kiarii, Poomani Penny Govender, Sara Ranjbari, Morteza Rezapour, Yasin Orooji, The role of magnetite/graphene oxide nano-composite as a high-efficiency adsorbent for removal of phenazopyridine residues from water samples, an experimental/theoretical investigation, J. Mol. Liq. 298 (2020), 112040. .
[12] F. Wang, Q. Li, D. Xu, Recent progress in semiconductor-based nanocomposite photocatalysts for solar-to-chemical energy conversion, Adv. Energy Mater. 7 (2017) 1700529(1–19.
[13] V. Kumaravel, S. Mathew, J. Bartlett, S.C. Pillai, Photocatalytic hydrogen production using metal doped TiO_2: a review of recent advances, Appl. Catal. B Environ. 244 (2019) 1021–1064.
[14] D. Lu, O.A. Zelekew, A.K. Abay, Q. Huang, X. Chen, Y. Zheng, Synthesis and photocatalytic activities of a CuO/TiO_2 composite catalyst using aquatic plants with accumulated copper as a template, RSC Adv. 9 (2019) 2018–2025.
[15] M.A. Kanjwal, N.A.M. Barakat, F.A. Sheikh, H.Y. Kim, Electronic characterization and photocatalytic properties of TiO_2/CdO electrospun nanofibers, J. Mater. Sci. 45 (2010) 1272–1279.
[16] M. Wang, Y. Hu, J. Han, R. Guo, H. Xiong, Y. Yin, TiO_2/NiO hybrid shells: p–n junction photocatalysts with enhanced activity under visible light, J. Mater. Chem. A 3 (2015) 20727–20735.
[17] K. Chockalingam, A. Ganapathy, G. Paramasivan, M. Govindasamy, A. Viswanathan, NiO/TiO_2 nanoparticles for photocatalytic disinfection of bacteria under visible light, J. Am. Chem. Soc. 94 (2011) 2499–2505.
[18] S. Rajendran, et al., Influence of mesoporous defect induced mixed-valent NiO (Ni^{2+}/Ni^{3+})-TiO_2 nanocomposite for non-enzymatic glucose biosensors, Sensors Actuators B Chem. 264 (2018) 27–37.
[19] R. Saravanan, et al., Mechanothermal synthesis of Ag/TiO_2 for photocatalytic methyl orange degradation and hydrogen production, Process Saf. Environ. Prot. 120 (2018) 339–347.
[20] R. Saravanan, J. Aviles, F. Gracia, E. Mosquera, Vinod Kumar Gupta, Crystallinity and lowering band gap induced visible light photocatalytic activity of TiO_2/CS (chitosan) nanocomposites, Int. J. Biol. Macromol. 109 (2018) 1239–1245.
[21] S. Contarini, G. Giunta, S. Loreti, N. Nistico, E. Lambers, P.H. Holloway, Interface analysis of ceramic matrix composites by XPS, AES, SEM and XRD, Surf. Interface Anal. 22 (1994) 258–262.

[22] H.T. Das, K. Mahendraprabhu, T. Maiyalagan, P. Elumalai, Performance of solid-state hybrid energy-storage device using reduced graphene-oxide anchored sol-gel derived Ni/NiO nanocomposite, Sci. Rep. 7 (2017), 15342. .
[23] S. Choudhury, D. Morgan, B.P. Uberuaga, Massive interfacial reconstruction at misfit dislocations in metal/oxide interfaces, Sci. Rep. 4 (2014) 6533.
[24] N.A.A. Samad, C.W. Lai, K.S. Lau, S.B.A. Hamid, Efficient solar-induced photoelectrochemical response using coupling semiconductor TiO_2-ZnO nanorod film, Materials 9 (2016) 937.
[25] K.F. Kalz, et al., Future challenges in heterogeneous catalysis: understanding catalysts under dynamic reaction conditions, ChemCatChem 9 (2017) 17–29.
[26] Y. Kang, et al., An amorphous carbon nitride photocatalyst with greatly extended visible-light-responsive range for photocatalytic hydrogen generation, Adv. Mater. 27 (2015) 4572–4577.
[27] A.E. Morales, I.I.R. López, M.R. Peralta, L. Tepech-Carrillo, M. Sánchez-Cantú, J.E. Moreno-Orea, Automated method for the determination of the band gap energy of pure and mixed powder samples using diffuse reflectance spectroscopy, Heliyon 5 (2019), e01505. .
[28] Y.Y. Gurkan, E. Kasapbasi, N. Turkten, Z. Cinar, Influence of se/N codoping on the structural, optical, electronic and photocatalytic properties of TiO_2, Molecules 22 (2017) 414.
[29] K.M. Reza, A. Kurny, F. Gulshan, Parameters affecting the photocatalytic degradation of dyes using TiO_2: a review, Appl Water Sci 7 (2017) 1569–1578.
[30] B. Neppolian, H.C. Choi, S. Sakthivel, B. Arabindoo, V. Murugesan, Solar light induced and TiO_2 assisted degradation of textile dye reactive blue 4, Chemosphere 46 (2002) 1173–1181.
[31] W. Zhao, W. Ma, C. Chen, J. Zhao, Z. Shuai, Efficient degradation of toxic organic pollutants with $Ni_2O_3/TiO_{(2-x)}B_x$ under visible irradiation, J. Am. Chem. Soc. 126 (2004) 4782–4783.
[32] S. Hu, F. Li, Z. Fan, The synergistic effect of nitrogen and Ni_2O_3 over TiO_2 photocatalyst in the degradation of 2,4,6-Trichlorophenol under visible light, Bull. Kor. Chem. Soc. 33 (2012) 4052–4058.